Synthesis and Application of Core–Shell Particles as Toughening Agents for Epoxies

JULIE Y. QIAN,[1,2] RAYMOND A. PEARSON,[1,3] VICTORIA L. DIMONIE,[1] and MOHAMED S. EL-AASSER[1,2,*]

[1]Emulsion Polymers Institute, [2]Chemical Engineering Department, and [3]Materials Science and Engineering Department, Lehigh University, Bethlehem, Pennsylvania 18015

SYNOPSIS

Poly(butadiene-*co*-styrene) [P(B–S)] core–poly(methyl methacrylate) (PMMA) shell particles were prepared using a two-step emulsion polymerization. These core–shell particles were used to toughen an epoxy polymer. The role of particle–epoxy interfaces were studied by systematically varying the shell compositions of the core–shell particles such as PMMA, P[MMA–acrylonitrile (AN)], P[MMA–glycidyl methacrylate (GMA)] and P[MMA–divinyl benzene(DVB)]. Therefore, the nature of the particle–epoxy interfaces is varied in terms of physical interactions and chemical bonding. The fracture toughness values of the toughened epoxies were measured using linear elastic fracture mechanics. Results indicate that the morphology of the dispersed particles in the epoxy matrix plays an important role in the toughening of epoxies. This degree of dispersion can be varied by incorporating AN and GMA comonomers in the PMMA shells or by crosslinking the shell. In summary, nanoscale interactions of the rubber–matrix interface do not directly influence fracture toughness, instead, it was found that the nanoscale interactions could be used to control the blend morphology which has a dramatic effect on toughness. © 1995 John Wiley & Sons, Inc.

INTRODUCTION

According to studies on the toughening mechanism of rubber-toughened epoxies,[1,2] the parameters that influence the toughening efficiency of the rubber-toughened epoxy system are: (1) properties of rubber particles such as size,[3] morphology,[4,5] and crosslink density of the rubber phase,[6,7] (2) the inherent ductility of epoxy matrix, e.g., crosslink density of the epoxy matrix,[8–10] (3) particle–epoxy interface.[11–14] Among these various factors, knowledge about the effect of the particle–matrix interface on toughening is still quite limited, and results from different groups are conflicting. Some groups claim that the interfacial adhesion between the rubber particle and epoxy matrix does not effect the fracture toughness of the modified epoxies,[11] while the others conclude that introducing chemical bonds between the rubber particles and epoxy matrix dramatically improves the fracture toughness of the modified epoxies.[12,13]

Telechelic poly(butadiene-*co*-acrylonitrile) copolymers with different terminating groups such as carboxyl (CTBN), amine (ATBN), and epoxy (ETBN) are most frequently used in these studies. In such toughened-epoxy systems, the rubber particles are formed due to the phase separation during the curing process, therefore the factors that might influence the fracture toughness of modified epoxies such as size, morphology, and composition are interdependent.[14–19] The problem of the interdependency can be solved by using core–shell latex particles,[3,12,20] since the size, morphology, composition, shell thickness, and crosslink density of the rubbery cores can be controlled separately by employing emulsion polymerization techniques.[21–23] Therefore, the effects of such parameters on the toughening of epoxies can be investigated individually.

The control of the particle parameters by emulsion polymerization has been extensively studied, and various efficient technologies have been developed. Monodisperse latex particles with a diameter

* To whom correspondence should be addressed.

Journal of Applied Polymer Science, Vol. 58, 439–448 (1995)
 CCC 0021-8995/95/020439-10

from submicron to micron range can be prepared by conventional emulsion polymerization, sequential seeded emulsion polymerization,[24] sequential swelling process,[25] and dispersion polymerization.[26-28] Cohesive strength which is influenced by crosslinking density of the rubber phase can be controlled by the conversion of polymerization[29] and the amount of the crosslinking agent.[30] Interfacial architecture can be controlled by changing the following parameters: (1) thickness of the shell which depends on the ratio of shell–core materials and polymerization mechanism; (2) chemical bonding and physical interaction between particles and matrix which can be enhanced by introducing functional groups onto the surface of shell; (3) grafting between the shell and core,[30,31] and (4) molecular weight of shell materials. Various morphologies of the composite such as core–shell, occluded, or multilayer can be achieved through two or multiple-stage emulsion polymerization.[23,32,33] Typically, core–shell morphology latex particles can be made by semicontinuous process under a monomer "starved" condition.[34-37]

The purpose of this work is to investigate the effects of the particle–epoxy interface on the toughening of epoxies. The particle–epoxy interfaces were varied in terms of physical interaction, chemical bonding, and extent of these interactions by varying the shell compositions of the core–shell particles such as poly(methyl methacrylate (PMMA), P(MMA–acrylonitrile [P(MMA–AN)], P(MMA–glycidyl methacrylate [P(MMA–GMA)], and P(MMA)–divinyl benzene [P(MMA–DVB)]. A low crosslink diglycidyl ether of bisphenol-A (DGEBA)–piperidine epoxy system was chosen as matrix, and therefore, more sensitivity to the improved fracture toughness is expected.[8-10]

EXPERIMENTAL

Materials

Tables I and II list materials used in preparation of rubber core latex particles and the corresponding core–shell latex particles. Styrene, methyl methacrylate, acrylonitrile, glycidyl methacrylate, and divinyl benzene monomers (Polysciences) were washed with a 10% aqueous solution of sodium hydroxide and passed through specific inhibitor remover columns (Aldrich) to remove different inhibitors. Butadiene (Matheson) was passed through a column of Ascarite to remove the inhibitor. Distilled-deionized (DDI) water was used in all experiments. All other materials were used without further purification: Nonylphenoxy poly(ethyleneoxy) ethanol 100 and 15 mol ethylene oxide (Igepal CO-990, Igepal CO-730, Rhone-Poulenc Inc.), dihexylester of sodium sulfosuccinate (Aerosol MA, American Cyanamid) surfactant, 2,2-azobis(2,4-dimethylvaleronitrile (Vazo-52, Dupont) initiator, piperidine curing agent (Fischer), and diglycidyl ether of bisphenol-A epoxy (DER 331, Dow Chemicals).

Table I Emulsion Polymerization Recipe for (B–S) Seed Latexes (Batch Process, 48 h at 60°C)

Materials	Amount (g)
Butadiene	20.0
Styrene	5.0
Igepal CO-990 or CO-730	Varied
Vazo-52	0.2
DDI water	71.2

Table II Seeded Emulsion Polymerization Recipe for P(B–S) Core–PMMA Shell Latex Particles (Semicontinuous Process, 5 h at 60°C)

Materials	Amount (g)
P(B–S) seed	12.50
MMA + AN (or GMA, or DVB)	12.50
Igepal CO-990	Varied
Potassium persulfate	0.20
DDI water	75

Preparation of Core–Shell Latex Particles

A two-stage emulsion polymerization process was used to prepare the poly(butadiene-co-styrene [P(B–S)] core–PMMA shell particles. The recipes and polymerization conditions are shown in Tables I for the seed latex particles and in Table II for the core–shell latex particles.

The polymerization for P(B–S) seed latex particles by batch process were carried out in pressure bottles within a constant temperature waterbath by end-over-end tumbling at 16 rpm. The following preparation procedure was followed: The bottles were first charged with all the ingredients expect butadiene, i.e., DDI water, emulsifier (or stabilizer), styrene, and initiator. The solution was purged with nitrogen for 5 min and cooled down with a salt–ice mixture. Then the liquid butadiene which was condensed with a mixture of liquid nitrogen and isopropanol was added into the bottle in a slight excess. The bottle was immediately capped with a crown metal cap which was laid with a neoprene gasket.

The excess butadiene was removed through a syringe needle.

The seeded polymerization of shell monomer by semicontinuous process were carried out in a stirred reactor fitted with a stirrer, condenser, nitrogen inlet tube, and a syringe pump with adjustable feed rates to feed the monomer through an inlet tube. The seed latex, emulsifier, and initiator were dissolved in the DDI water and the solution was heated to 60°C with stirring under nitrogen. The shell monomers which contain specific ratios of MMA and functional comonomers were premixed and then added to the aqueous phase over a 2-h period under a steady stream of nitrogen. Finally, the reactions were allowed to continue for additional 3 h more to polymerize all the residual monomer.

The synthesized P(B–S) core–PMMA shell latex particles were freeze-dried to ensure that the particles did not segregate during the drying process.

Characterization of Core–Shell Particles

The size and size distribution of both P(B–S) seed latex particles and P(B–S) core–PMMA shell latex particles were measured using a Nicomp submicron particle sizer and a Phillips 400 transmission electron microscope, combined with a Ziess mop counter which allows one to measure the average particle size and size distribution by counting a large number of particles on the micrographs. The sizes of the core–shell particles determined by the TEM measurement were compared to the values calculated based on weight ratios of secondary stage monomer–seed polymer (M–P).

The morphology of the P(B–S) core–PMMA shell particles with various shell compositions were examined also in a Phillips 400 transmission electron microscope. The P(B–S) core–PMMA shell particles were first positively stained with OsO_4, and then negatively stained with phosphotungstic acid (PTA) to delineate the core–shell morphology.

Preparation of Rubber-Modified Epoxies

To disperse the dried core–shell latex particles into the epoxy matrix, the following procedure was used: The particles were added into the epoxy and the system was mixed by a mechanical stirrer at 250 rpm. The mixture was then heated to 80°C and degassed. Finally, a curing agent (piperidine) was added while slowly stirring. The mixture was again degassed and poured into a preheated mold at 120°C. The mold was placed in an air-circulating oven at 120°C for 16 h. After this time, the mold was removed from the oven and allowed to cool gradually to room temperature.

Evaluation of Mechanical Behavior

The fracture toughness was measured according to the ASTM D5045-91 protocol. The critical stress intensity factor K_{IC} was determined using a single-edge-notched-type specimen (6.4 × 12.7 × 80 mm) in a three-point bending geometry (SEN-3PB). The tests were performed using an Instron 1011 test machine equipped with a 100-lb load cell; the crosshead rate was 1 mm/min. A minimum of five specimens were used to ensure the accuracy. The critical stress intensity factor was calculated using the following relationships:

$$K_{IC} = Y\frac{3PSa^{1/2}}{2tw^2} \quad (1)$$

where P is the critical load for crack propagation, S is the length of the span, a is the crack length, t is the thickness, w is the width, and Y is a nondimensional shape factor given by

$$Y = 1.9 - 3.07\,(a/w) + 14.53\,(a/w)^2 - 25.11\,(a/w)^3 + 25.8\,(a/w)^4 \quad (2)$$

The effect of crack tip plasticity on the validity of the K measurements could be eligible if the thickness is large enough to provide plane constraint.

$$t > 2.5(K_{IC}/\sigma_y) \quad (3)$$

Tensile properties were measured according to the ASTM D638 guideline. Type I dogbone specimens were machined from the cured plaques. The specimens were tested using a screw-driven Instron testing frame at crosshead speed of 5 mm/min. A clip-on extensometer was used to measure strain in the specimen gauge length. Results are an average of three specimens.

Scanning Electron Microscopy

The degree of the dispersability of the particles in the epoxy matrix were examined by scanning electron microscopy (SEM) of the fracture surfaces of the SEN-3PB specimens examined using a Joel 6300 scanning electron microscope. The samples were coated with a thin layer of gold-palladium to reduce any charge buildup on the surface.

RESULTS AND DISCUSSION

P(B–S) core–PMMA Based Shell Latex Particles

Monodisperse P(B–S) seed latex particles in the size range from 80 to 300 nm were prepared by conventional emulsion polymerization techniques. Different types of emulsifiers were used, including Igepal CO-990, Igepal CO-730, and Aerosol MA. The results are shown in Table III. Aerosol MA can be used to produce seed particles with a size smaller than 100 nm in diameter. Igepal CO-990 was used to produce seed particles in the size range from 80 to 120 nm in diameter. Latex particle with size range larger than 150 nm in diameter can be prepared with Igepal CO-730. The reason we choose Aerosol MA in the seed preparation is that it was expected to produce small size particles if used alone, and large particles if combined with other electrolytes. Furthermore, it can reduce the tendency for producing a secondary crop of particles in the shell preparation, and latex cleaning is not too difficult, since it is an anionic emulsifier. However, in our experiments, the addition of electrolytes such as sodium chloride and sodium bicarbonate seemed to have no obvious effect on the particle size. Furthermore, as the size of P(B–S) latex particles reached to a certain value (around 300 nm), the polymerization conversion became incomplete (approximately 50%). An increase in the reaction time and a second shot of the initiator did not result in any increase in the polymerization conversion. The underlying reasons for this observation are still not clear.

The use of Igepal CO-990 emulsifier is preferred based on our results on the preparation of the core–shell particles: (1) The cleaning step before the shell preparation can be avoided when the emulsifier concentration used in seed preparation is lower than 3% (based on the total weight). (2) No additional emulsifier is needed for the shell preparation, therefore, the amount of the emulsifier in the final core–shell particles can be kept at minimum level. (3) Compared to Dowfax 2A1 emulsifier (sodium disulfonated lauryl alkylated diphenyloxide, Dow Chemicals),[38] which is a common emulsifier for latex preparation, the critical amount of Igepal CO-990 (i.e., the minimum concentration at which the latex is free of coagulum) is insensitive to the ratios of the secondary monomer and seed polymer (M–P), and consistent with the calculated values based on the consideration of the surface area of the particles; and this is more desirable in a semicontinuous process.

Table III Size and Size Distribution of P(B–S) Latex Particles Prepared with Different Emulsifiers at Various Concentrations

	[E] (%)[a]				
	Aerosol MA				
	9.6	4.8	2.4	1.2	0.6
D_n (nm)[a]	Bimodal	49.7	90.3	122.0	168.9
D_v (nm)[a]		64.1	99.4	153.0	222.0
S.D. (%)		28.8	17.7	26.1	26.3
	Igepal CO-990				
	9.0	6.0	4.5	3.0	1.5
D_n (nm)[a]	Bimodal	78.5	88.7	100.9	Coagulated
D_v (nm)[a]		89.1	90.0	110.8	
S.D. (%)		21.2	18.9	17.4	
	Igepal CO-730				
		3.0		1.3[b]	0.75[b]
D_n (nm)[a]		106.7		224.6	232.0
D_v (nm)[a]		136.3		300.7	305.7
S.D. (%)		27.0		26.9	26.3

[a] [E] (%) = wt % emulsifier based on total recipe; D_n = number-average of particle diameter; D_v = volume-average of particle diameter.

[b] The polymerizations were not complete.

Figure 1 displays the transmission electron micrographs of P(B–S) seed latex particles prepared with Igepal CO-990 and Igepal CO-730 emulsifiers with two different sizes. One can see that the particle size distributions in both cases were quite narrow. The P(B–S) latex particles used as seed for the seeded emulsion polymerization were prepared with Igepal CO-990 at a concentration of 3 wt %, with a diameter of 84 nm.

Several comonomers were chosen to be incorporated into the PMMA shell. Acrylonitrile was expected to increase physical interaction between the particles and epoxy matrix based on its higher polarity; GMA which has an epoxide functional group might introduce a chemical bonding between the particles and epoxy matrix through the reaction between epoxide group and curing agent; DVB was used as crosslinker to the PMMA shell, so as to increase the chemical bonds in the PMMA shell. The effects of incorporating these functional comonomers on the stability of the latexes and morphologies were first evaluated in a batch process. Compared with the homopolymer PMMA, the latex prepared with AN comonomer was more stable even at higher polymerization temperatures. GMA and DVB

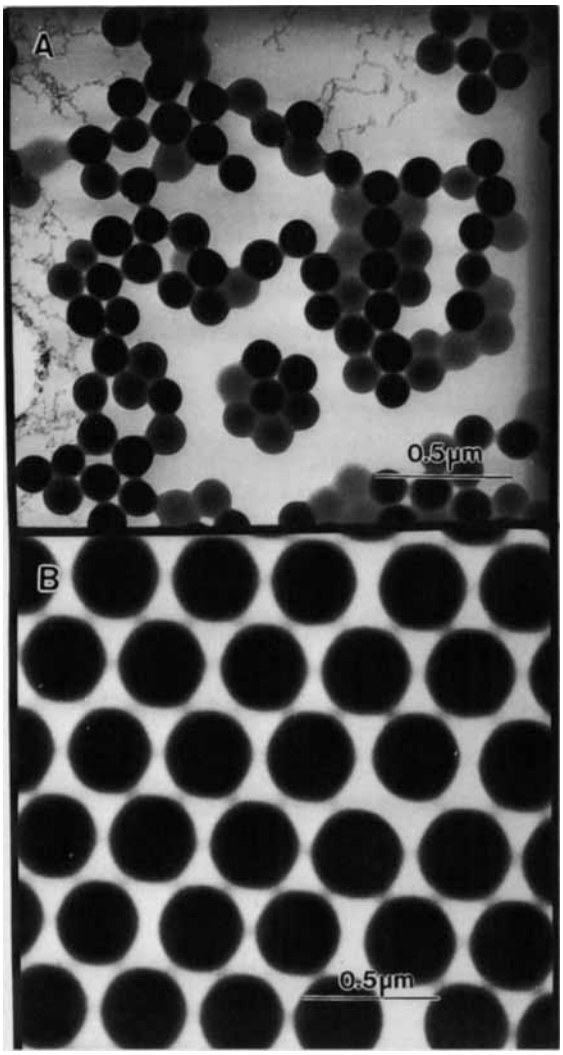

Figure 1 Transmission electron micrographs of P(B–S) seed latex particles with two different sizes stained with OsO_4: (A) D = 84 nm; (B) D = 300 nm.

seemed to have no obvious influence on the stability of the latexes. Then the optimal polymerization conditions were applied in the semicontinuous process.

Figure 2 is the transmission electron micrographs of P(B–S) core–PMMA shell latex particles with various shell compositions including PMMA, P(MMA–AN), P(MMA–GMA), and P(MMA–AN–DVB). The P(B–S) cores which were stained with OsO_4 appear dark, and the shell materials which were negatively stained with PTA appear light. In all cases, uniform core–shell morphologies were observed. The effect of crosslinking agent (DVB) on the morphology of the core–shell particles is shown to be significant by comparing the TEM micrographs in the Figure 2(D) with the others in Figure 2. In the case of the core–shell particle with DVB in the shell material, a more uniform and full coverage of the core particles by the shell material was observed. This is because the tendency of phase separation of the shell polymer from core polymer is suppressed due to the decrease of chain mobility of the PMMA molecules by the presence of crosslinks.

Mechanical Behavior of Modified Epoxies

The mixing conditions for dispersing of the dried core–shell particles into the epoxy matrix were varied in terms of rate and time of mechanical stirring. Table IV shows the effect of mixing process on the mechanical behaviors of the epoxy modified with the core–shell particles having a homo-PMMA shell. The stirring rate was varied in the range of 100–250 rpm, and stirring time was changed in the range of 2–3 h. It could be expected that the higher stirring rate and longer stirring time would result in a better degree of dispersion of the particles in the epoxy matrix. The results shown in Table IV indicate that the modified epoxies having a better particle dispersion exhibited much higher fracture toughness, while their yield stress (σ_y) and modulus (E) remained at the same values. Therefore, mixing conditions which provided a higher toughness (i.e., 250 rpm and 3 h) were applied to prepare all the rubber-modified epoxies.

The effect of the shell composition of the core–shell particles on the toughness of the modified epoxy is illustrated in Table V. Knowing that the K_{IC} value of the neat epoxy is 0.78 MPa $m^{1/2}$, and the K_{IC} values of the epoxies modified with CTBN rubber particles are usually around 2.0 MPa $m^{1/2}$ [3], one can see that the K_{IC} values of the epoxies modified with 10% by volume rubber of our custom-made core–shell particles were successfully increased to the range of 2.4–2.7 MPa $m^{1/2}$. Young's modulus and the yield stress decreased as expected and seemed to have no significant dependence on the shell composition, which indicates that the variation of the shell composition did not change the properties of the P(B–S) cores.

The K_{IC} values in Table V indicate that incorporation of both AN and GMA functional comonomers in PMMA shells does not improve the fracture toughness of the toughened epoxies. The fracture toughness of the epoxies modified with the core–shell particles containing a homo-PMMA shell is slightly higher than that with copolymer shells. Furthermore, close K_{IC} values were observed for the epoxies toughened with the particles containing a AN comonomer shell and a GMA comonomer shell,

indicating that the physical interaction versus the chemical bonding between the particles and epoxy matrix on the fracture toughness of the modified epoxies are not significant. However, according to the recent study by Kling and Ploehn,[39] the epoxy rings in GMA can be opened by the crosslinking side reactions or through hydrolysis by water during the seeded emulsion polymerization, and survival ratios for these epoxy groups after the polymerization are in the average of 60%. Therefore, the epoxy groups that survived in the shells might not be enough to provide sufficient chemical bonding between the particles and the epoxy matrix. The K_{1C} value of the epoxy modified with the particles with a crosslinked shell is significantly lower than that without crosslinked shell, indicating that crosslinking of the shell suppresses the improved fracture toughness of the toughened epoxies. These results will be further discussed in next section.

Table IV Effect of Mixing Process on the Mechanical Behavior of the Modified Epoxies

Shell Composition	Time (h)	rpm	K_{IC} (MPa $m^{1/2}$)	E (GPa)	σ_y (MPa)
PMMA	2	100	1.66 ± 0.15	2.8	64.0
PMMA	3	250	2.69 ± 0.02	2.7	64.7

Fracture Surface Inspection

Figure 3 presents the scanning electron micrographs taken from the fracture surface of SEN-3PB spec-

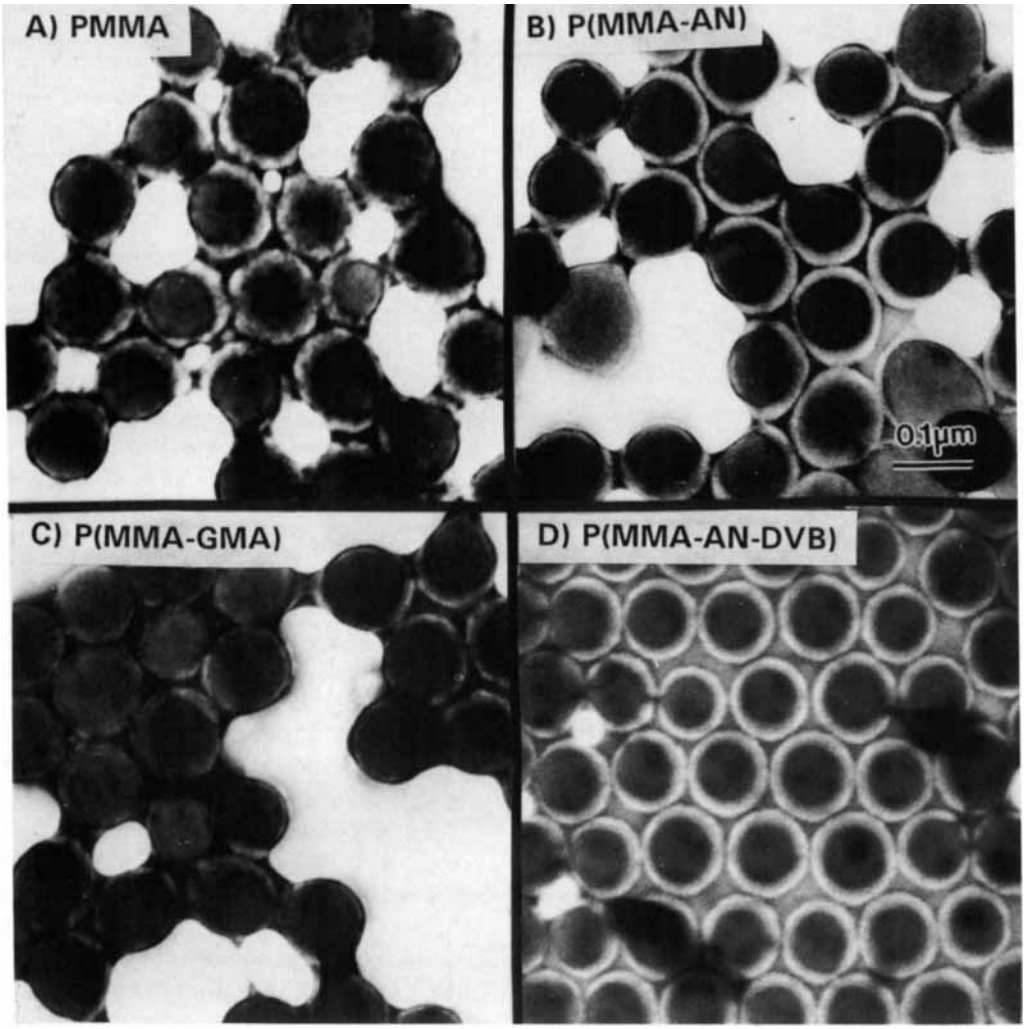

Figure 2 Transmission electron micrographs of P(B–S) core–PMMA shell latex particles prepared by a semicontinuous seeded emulsion polymerization process, and positively stained with OsO_4, and negatively stained with PTA.

Table V Effect of Shell Composition on Mechanical Behaviors of Rubber-Modified Epoxies

Shell Composition	K_{1C} (MPa $m^{1/2}$)	E (GPa)	σ_y (MPa)
PMMA	2.69 ± 0.02	2.7	64.7
P(MMA–AN) (90/10)	2.57 ± 0.02	2.9	66.1
P(MMA–GMA) (90/10)	2.45 ± 0.07	—	—
P(MMA–DVB) (95/5)	2.49 ± 0.04	2.7	68.1
Neat epoxy	0.78 ± 0.10	3.0	75.5
CTBN-8[3]	2.10	2.6	63

imens in the stress-whitened zone. The effect of the mixing conditions on the disperse morphology of the particles in the epoxy matrix was apparent. When a slow stirring rate of 100 rpm and a short mixing time of 2 h were used in the mixing process, the overall dispersability of the particles in the epoxy was not uniform, and huge aggregates of particles can be visually seen. The SEM examination, as illustrated in Figure 3(A), showed that a large number of particles were found in one area, while no particles was observed in the other areas. The size of these aggregates corresponded to that of particle aggregates formed in the freeze-drying process. This suggests that the particles were not able to be separated from each other during the mixing process. In other words, there existed no epoxy matrix between those particles, therefore, there could be no particle–epoxy interfaces within these aggregates. When the stirring rate and mixing time were increased to 250 rpm and 3 h, the overall dispersability of the particles in the epoxy matrix became more homogeneous, although the particles still microsegregated into clusters, as shown in Figure 3(B). The particles were able to be separated from their original powder form, and uniformly redistributed in the epoxy matrix. Therefore, all particles were surrounded by the epoxy matrix and there existed a rubber–epoxy interface between the individual particles within the clusters.

As already shown in Table IV, the rubber-modified epoxy with a overall uniform dispersion of the particles had a much higher fracture toughness than the rubber-modified epoxy containing large aggregates, as listed in Table IV. Two significant pieces of information can be obtained from these results: (1) the overall uniform concentration of the dispersed particles in the epoxy matrix is essential for high toughness; (2) the rubber–epoxy interface plays a very important role in controlling uniformity of morphology.

Figure 4 presents the scanning electron micrographs of the fracture surfaces of the epoxies prepared at better mixing conditions (i.e., 250 rpm and 3 h) in the stress-whitened zone. A segregated morphology in which particles clustered into individual "islands" in the epoxy matrix was observed in all the cases. Furthermore, these particles were still separated from each other by the epoxy matrix.

The effect of the shell composition of the core–shell particles on the degree of dispersability of the particles in the epoxy matrix is significant, as shown in Figure 4. In the case of the core–shell particles containing a homo-PMMA shell, the segregation of the particles was more severe, where the cluster size was approximately in the range of 3–5 μm, as illustrated in Figure 4(A). The cluster size was reduced to about 1–3 μm when DVB (crosslinker) was introduced to the shell, as shown in Figure 4(B). In the cases of the core–shell particles containing AN

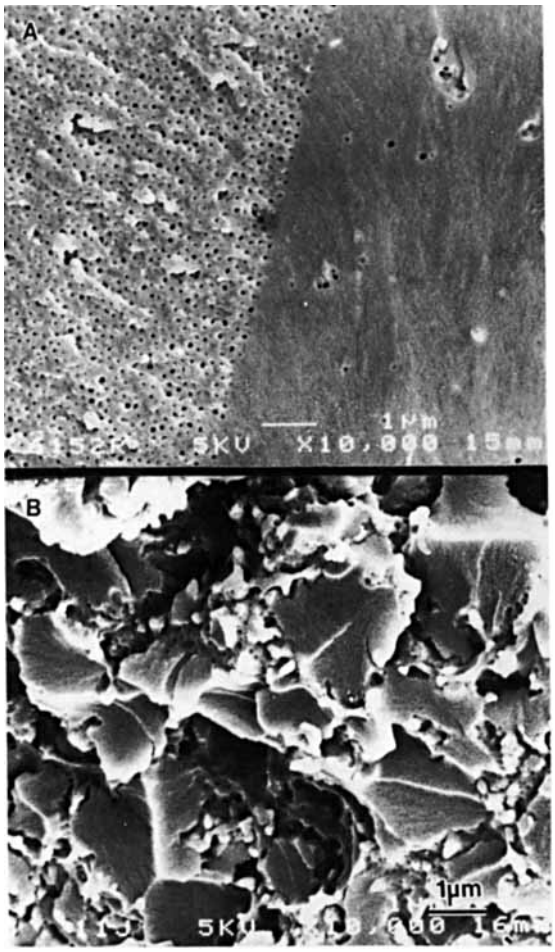

Figure 3 Scanning electron micrographs of the fracture surfaces of the epoxies modified with custom made core–shell particles in different mixing conditions: (A) rpm = 100, time = 2 h; (B) rpm = 250, time = 3 h.

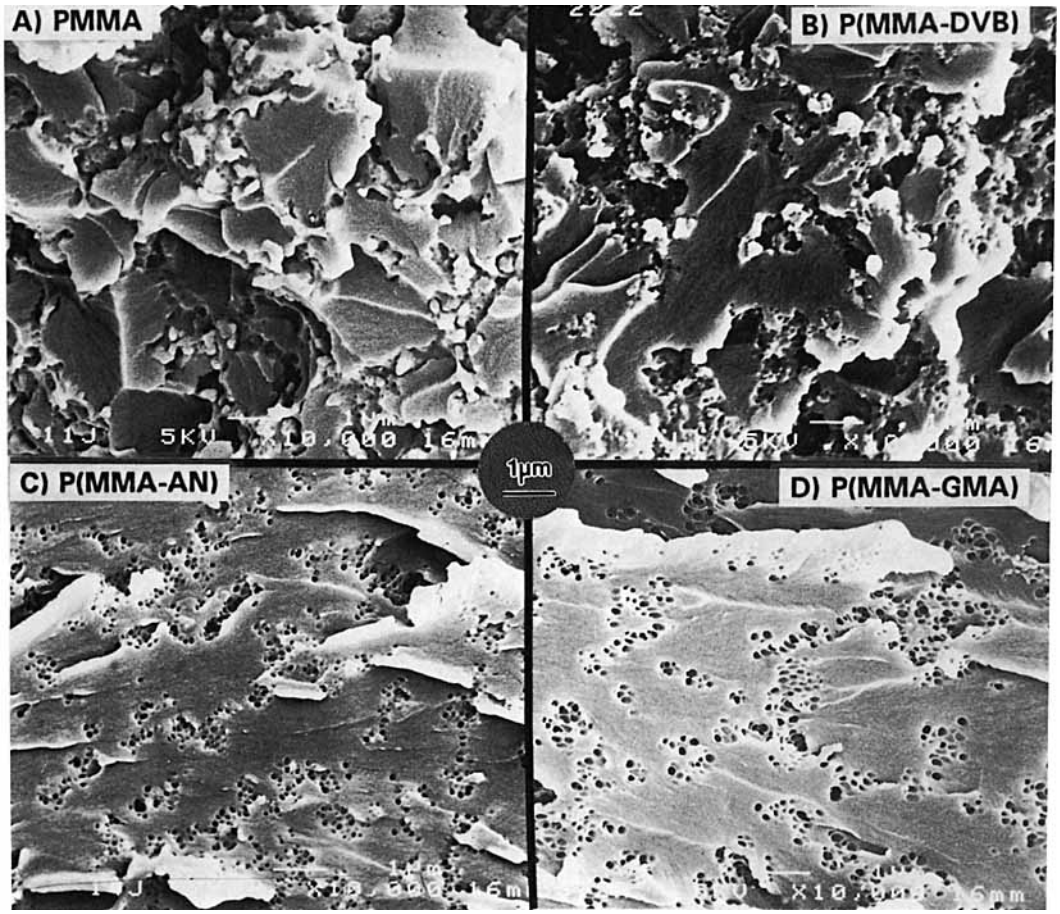

Figure 4 Scanning electron micrographs of the fracture surfaces of the epoxies modified by the core–shell particles with different shell compositions: (A) PMMA 100%; (B) P(MMA–DVB) 95:5; (C) P(MMA–AN) 90:10; (D) P(MMA–GMA) 90:10.

or GMA comonomers in the shell, the cluster sizes were nearly identical, about 1–2 μm, as displayed in Figures 4(C) and 4(D). This suggests that the degree of dispersability of the core–shell particles in the epoxy can be improved by increasing the rigidity of the shell (crosslinking) or by enhancing the particle–epoxy interfacial interactions through some chemical bonding or physical interaction.

Correlating the particle-dispersed morphology in the epoxy matrix with the fracture toughness of the modified epoxies, as listed in Table V, reveals that the degree of particle dispersability in the epoxy matrix plays a crucial role in toughening of epoxies. A higher degree of segregation (clustering) of the particles in the epoxy matrix yields a higher fracture toughness of the modified epoxies. A similar disperse morphology results in close K_{IC} values, independent of the shell composition, as evidenced by the cases with AN and GMA comonomers or DVB crosslinker in the shells.

The examination by atomic force microscopy (AFM) of the fracture surfaces of the modified epoxies have shown the rubber particles were all internally cavitated. Furthermore, the degree of these cavitations is strongly dependent on the crack mode; the size of the cavities in a stress-whitened zone were much larger than that in a fast crack growth region.

CONCLUSIONS

Model P(B–S) core–PMMA shell particles with uniform shell and various shell compositions can be prepared by two-step emulsion polymerization. Igepal CO-990 was chosen as emulsifier for both seed and shell preparation, and the amount of the emulsifier in the resulted core–shell particles was kept at a minimum level. The addition of the crosslinking agent in the shell materials results in a more uni-

form, dense layer with full coverage of the cores by the shell material.

The fracture toughness of the epoxies was successfully improved by the custom-made core–shell particles as evidenced by the increase of K_{IC} value from 0.78 to 2.69 MPa $m^{1/2}$. The toughening mechanism was found to be internal cavitation of rubber particles and concomitant matrix shear yielding. This mechanism has been observed previously in CTBN-modified epoxies. However, it was found that the extent of dispersion of the particles in the epoxy matrix plays a crucial role in toughening epoxies. Microsegregation of the particles in the epoxy matrix appears to be desirable to achieve optimal fracture toughness. The degree of dispersability of the particles in epoxy can be influenced by incorporation of a small amount of AN or GMA comonomer or by crosslinking of the shell. The role of the dispersed morphology on the toughness was further investigated by systematically varying AN–MMA ratios in the shell and it will be discussed in the subsequent study. It was found that the dispersed particle morphology can be precisely controlled by the AN content in PMMA shell. Again, the clustering morphology yields a much higher toughness than a uniform morphology.

Financial support for this project from Emulsion Polymers Institute Liaison Program at Lehigh University, NSF-RI Grant No. MSS-9211664, and ACS-PRF Grant No. 25033-G7P is gratefully acknowledged.

REFERENCES

1. A. C. Garg and Y. W. Mai, *Comp. Sci. Technol.* **31,** 179 (1988).
2. Y. Huang, D. L. Hunston, A. J. Kinloch, and C. K. Riew, in *Toughened Plastics I,* C. K. Riew and A. J. Kinloch, Eds., ACS Ser., **233,** 1 (1993).
3. R. A. Pearson and A. F. Yee, *J. Mater. Sci.,* **26,** 3828 (1991).
4. P. A. Lovell, J. McDonald, D. E. J. Saunders, M. N. Sherratt, and R. J. Young, in *Toughened Plastics I,* C. K. Riew and A. J. Kinloch, Eds., ACS Ser., **233,** 61 (1993).
5. A. C. Archer, P. A. Lovell, J. McDonald, M. N. Sherratt, and R. J. Young, *Polym. Mater. Sci. Eng.,* **70,** 153 (1994).
6. D. Li, X. Li, and A. F. Yee, *Polym. Mater. Sci. Eng.,* **63,** 296 (1990).
7. R. Bagheri and R. A. Pearson, *Polym. Mater. Sci. Eng.,* **70,** 15 (1994).
8. C. Meets, *Polymer,* **15,** 675 (1974).
9. R. A. Pearson and A. F. Yee, *J. Mater. Sci.,* **24,** 2571 (1989).
10. S. H. Liu and E. B. Nauman, *J. Mater. Sci.,* **26,** 6581 (1991).
11. Y. Huang, A. J. Kinloch, R. J. Bertsch, and A. R. Siebert, in *Toughened Plastics I,* C. K. Riew and A. J. Kinloch, Eds., ACS Ser., **233,** 189 (1993).
12. H. J. Sue, E. I. Garcia-Meitin, D. M. Pickelman, and P. C. Yang, in *Toughened Plastics I,* C. K. Riew and A. J. Kinloch, Eds., ACS Ser., **233,** 259 (1993).
13. D. E. Henton, D. M. Pickelman, C. B. Arends, and V. E. Meyer, U.S. Pat. 4,778,851 (1988).
14. T. K. Chen and Y. H. Jan, *Polym. Eng. Sci.,* **31,** 577 (1991).
15. L. T. Manzione, J. K. Gillham, and C. A. McPherson, *J. Appl. Polym. Sci.,* **26,** 907 (1981).
16. R. J. J. Williams, J. Borrajo, H. E. Adabbo, and A. J. Rojas, in *Rubber-Modified Thermoset Resins,* C. K. Riew, J. K. Gillham, Eds., ACS Ser., **208,** 195 (1984).
17. R. J. J. Williams, J. Borrajo, H. E. Adabbo, and A. J. Rojas, in *New Polymeric Materials,* E. Martuscelli and C. Marchetta, Eds., VNU Science, Utrecht, 1987.
18. A. Vazquez, A. J. Rojas, H. E. Adabbo, J. Borrajo, and R. J. J. Williams, *J. Polym.,* **28,** 1156 (1987).
19. S. Montarnal, J. P. Pascault, and H. Sautereau, in *Rubber-Toughened Plastics,* C. K. Riew, Ed., ACS Ser., **222,** 193 (1989).
20. R. Mulhaupt, *Chimia, Chem. Rep.,* **44,** 43 (1990).
21. M. S. El-Aasser and R. M. Fitch, Eds., *Future Directions in Polymer Colloids,* NATO ASI Series E, **138** (1987).
22. E. S. Daniels, E. D. Sudol, and M. S. El-Aasser, Eds., *Polymer Latex, Preparation, Characterization and Applications,* ACS. Ser., **492,** (1992).
23. D. I. Lee, *ACS Sym. Ser.,* **165,** 893 (1981).
24. J. W. Vanderhoff, M. S. El-Aasser, F. J. Micale, E. D. Sudol, C. M. Tseng, A. Silwanowicz, H. R. Sheu, and D. M. Kornfeld, *Polym. Mater. Sci. Eng. Prep.,* **54,** 587 (1986).
25. J. Ugelstad, P. C. Mork, K. H. Kaggurud, T. Ellingsen, and A. Berge, *Adv. Colloid Interface Sci.,* **13,** 101 (1980).
26. K. E. J. Barrett, *Dispersion Polymerization in Organic Media,* Wiley, New York, 1975.
27. S. Shen, E. D. Sudol, and M. S. El-Aasser, *J. Polym. Sci., Part A: Polym. Chem.,* **32,** 1393 (1993).
28. M. D. Croucher, in *Future Directions in Polymer Colloids,* M. S. El-Aasser and R. M. Fitch, Eds., NATO ASI Series E, **138,** 209 (1987).
29. P. A. Weerts, *Emulsion Polymerization of Butadiene, A Kinetic Study,* Ph.D. Dissertation, Technische Universiteit Eindhoven, 25 (1990).
30. M. P. Merkel, V. L. Dimonie, M. S. El-Aasser, and J. W. Vanderhoff, *J. Polym. Sci., Part A: Polym. Chem.,* **25,** 1219 (1987).
31. M. P. Merkel, V. L. Dimonie, M. S. El-Aasser, and J. W. Vanderhoff, *J. Polym. Sci., Part A: Polym. Chem.,* **25,** 1755 (1987).
32. Y. C. Chen, V. L. Dimonie, and M. S. El-Aasser, *J. Appl. Polym. Sci.,* **42,** 1049 (1991).

33. J. L. Jonsson, H. Hassander, L. H. Jansson, and B. Tornell, *Macromolecules*, **24,** 126 (1991).
34. J. C. Daniel, *Makromol. Chem. Suppl.*, **10/11,** 359 (1985).
35. S. Lee and A. Rudin, in *Polymer Latex, Preparation, Characterization and Applications*, E. S. Daniels, E. D. Sudol, and M. S. El-Aasser, Eds., Symp. ACS, Ser. **492,** 234 (1992).
36. J. W. Vanderhoff, in *Future Directions in Polymer Colloids*, M. S. El-Aasser and R. M. Fitch, Eds., NATO ASI Series E, **138,** 23 (1987).
37. T. I. Min, A. Klein, M. S. El-Aasser, and J. W. Vanderhoff, *J. Polym. Sci., Polym. Chem.* **22,** 2845 (1983).
38. V. L. Dimonie, M. S. El-Aasser, and J. W. Vanderhoff, *Makromol. Chem., Macromol. Symp.*, **35/36,** 447 (1990).
39. J. A. Kling and H. J. Ploehn, *J. Polym. Sci., Part A: Polym. Chem.*, to appear.

Received October 8, 1994
Accepted February 6, 1995